Bollettino Unione Matematica Italiana

Daniele Boffi, Nicola Cavallini, Francesca Gardini, Lucia Gastaldi

Stabilized Stokes Elements and Local Mass Conservation

Bollettino dell'Unione Matematica Italiana, Serie 9, Vol. **5** (2012), n.3, p. 543–573.

Unione Matematica Italiana

<http://www.bdim.eu/item?id=BUMI_2012_9_5_3_543_0>

Bollettino dell'Unione Matematica Italiana, Unione Matematica Italiana, 2012.

Bollettino U. M. I.
(9) **V** (2012), 543-573

Stabilized Stokes Elements and Local Mass Conservation

D. Boffi - N. Cavallini - F. Gardini - L. Gastaldi

Dedicated to Enrico Magenes

Abstract. – *In this paper we discuss lowest order stabilizations of Stokes finite elements. We study the behavior of the constants in front of the error estimates in terms of the stabilization parameters and confirm with numerical tests that the bounds are sharp. Moreover, we investigate the local mass conservation properties of the considered schemes and analyze new schemes with enhanced pressure approximation, which guarantee a better local discretization of the divergence free constraint.*

1. – Introduction

Finite element simulations of fluid-dynamic phenomena require a good understanding of the approximation of Stokes problem. Several mixed finite element schemes are known for the solution of Stokes problem (see, e.g., [2] and the references therein) and a large amount of literature deals with the study of finite element choices satisfying the appropriate compatibility conditions for a correct approximation (the famous *inf-sup* condition). Similarly, numerous authors have discussed the use of non compatible finite element spaces combined with suitable stabilization techniques.

In this paper we present in a unified approach stabilized schemes originated by the addition of a term like $(\nabla p, \nabla q)$ and/or of a term involving the pressure jumps across the interelement boundaries. A stabilization technique of this kind was first proposed by Brezzi and Pitkäranta in [8] for the $P_1 - P_1$ triangular element. Then Hughes et al in [15, 14, 13] generalized this stabilization to deal with any pair of velocity and pressure approximations (see also [12] for a review on stabilized schemes).

In doing so, we recall the main steps of the convergence analysis. Particular care is paid to the identification of the constants in front of the error estimates as functions of the stabilization parameters. The aim is to see if it is possible to tune such parameters in order to maximize the rate of convergence in presence of non-smooth pressure solutions.

Another important feature of Stokes finite element schemes is their capabilities to enforce the divergence free condition in a robust way. This issue is strictly related to the mass conservation property which is of fundamental importance for applications, in particular for transient problems when coupled with other equations, like in fluid-structure interactions or in free-surface problems (see, for instance, [16, 19, 20, 11, 21, 22]). We have faced this problem, for instance, when dealing with the approximation of fluid-structure interaction problems and using the Immersed Boundary Method [6, 5, 3]. In particular, we have shown that a suitable modification of commonly used Stokes finite elements can prove very useful in order to enhance the local mass conservation [4]. The modification consists in adding piecewise constant functions to the space approximating the pressures. This has the natural effect of enforcing an averaged version of the divergence free condition locally on each element.

In this paper we analyze the pressure enhancement modification in the framework of stabilized finite elements.

The main consequence of the analysis is that the enhancement is poorly effective in the case of low order elements and non smooth data. In particular, if the polynomial order of the velocity space is not high enough (quadratic in 2D or cubic in 3D), then the pressure enhancement requires an appropriate stabilization involving the pressure jumps along the interelements. First of all, we observe that such stabilization destroys the local nature of the mass conservation property. Moreover, the stabilization term introduces a consistency error with reduced rate of convergence in case of non-smooth pressure solutions. This drawback applies, for instance, to the stabilized $P_1 - P_0$ element or to the enhanced version of the popular $P_1 - P_1$ stabilized element. In order to circumvent this phenomena we introduce a new finite element that combines the feasible characteristics of the $P_1 - P_1$ stabilized element and mass conservation properties of the Bercovier-Pironneau element.

In the next section we briefly recall the problem we are dealing with. Section 3 provides the analysis for the stabilized schemes and Section 4 discusses the local mass conservation properties of the proposed schemes, together with their enhanced counterpart. Several numerical tests are reported in Section 5.

2. – Problem setting

We consider the stationary Stokes problem

$$
\begin{aligned}
-\Delta \boldsymbol{u} + \nabla p &= \boldsymbol{f} && \text{in } \Omega,\\
\operatorname{div} \boldsymbol{u} &= 0 && \text{in } \Omega,\\
\boldsymbol{u} &= \boldsymbol{0} && \text{on } \partial\Omega,
\end{aligned}
\tag{1}
$$

where $\boldsymbol{u}$ is the fluid velocity, p the pressure, $\boldsymbol{f}$ the external force, and $\Omega \subset \mathbb{R}^n$ $(n = 2, 3)$ a polygonal or polyhedral domain.

Let $\boldsymbol{V} = H_0^1(\Omega)^n$ and $Q = L_0^2(\Omega) = \{q \in L^2(\Omega) : \int_\Omega q\, d\boldsymbol{x} = 0\}$, then the weak formulation of problem (1) reads:

$$\text{find } (\boldsymbol{u}, p) \in \boldsymbol{V} \times Q \text{ such that} \tag{2}$$
$$\begin{cases} a(\boldsymbol{u}, \boldsymbol{v}) + b(\boldsymbol{v}, p) = (\boldsymbol{f}, \boldsymbol{v}) & \forall \boldsymbol{v} \in \boldsymbol{V}, \\ b(\boldsymbol{u}, q) = 0 & \forall q \in Q, \end{cases}$$

where $(\cdot,\cdot)$ denotes the L^2-inner product, and $a(\cdot,\cdot)$ and $b(\cdot,\cdot)$ are the bilinear forms

$$a(\boldsymbol{u}, \boldsymbol{v}) = \int_\Omega \nabla \boldsymbol{u} : \nabla \boldsymbol{v}\, d\boldsymbol{x},$$

$$b(\boldsymbol{u}, p) = -\int_\Omega p \operatorname{div} \boldsymbol{u}\, d\boldsymbol{x}.$$

Let $\mathcal{T}_h$ denote a shape-regular family (i.e., satisfying the minimum angle condition, see [9]) of simplicial decompositions of Ω. As usual, we require that any two elements in $\mathcal{T}_h$ share at most a common face, edge, or vertex. We denote respectively by h_e, h_K, and h the length of the edge (face in three dimensions) e, the diameter of the element K, and the mesh size. Finally, $\mathcal{E}^I$ is the set of interior edges (faces in three dimensions) of the mesh.

Let $\boldsymbol{V}_h$ and Q_h be two conforming finite element subspaces of $\boldsymbol{V}$ and Q, respectively. The mixed approximation of problem (2) is given by:

$$\text{find } (\boldsymbol{u}_h, p_h) \in \boldsymbol{V}_h \times Q_h \text{ such that} \tag{3}$$
$$\begin{cases} a(\boldsymbol{u}_h, \boldsymbol{v}_h) + b(\boldsymbol{v}_h, p_h) = (\boldsymbol{f}, \boldsymbol{v}_h) & \forall \boldsymbol{v}_h \in \boldsymbol{V}_h, \\ b(\boldsymbol{u}_h, q_h) = 0 & \forall q_h \in Q_h. \end{cases}$$

It is well known (see [7]) that, since $a(\cdot,\cdot)$ is coercive on $\boldsymbol{V}$, for the discrete problem to be well-posed it is sufficient that the pair $(\boldsymbol{V}_h, Q_h)$ satisfies the so called "inf-sup stability condition". Conversely, conforming low order elements such as $P_1 - P_0$ (linear velocity, constant pressure) and $P_1 - P_1^c$ (linear velocity, continuous linear pressure) are known to be unstable.

3. – Stabilized formulations

We consider the stabilized formulation presented in [12] which, in an abstract setting, reads as follows:

$$\text{find } (\boldsymbol{u}_h, p_h) \in \boldsymbol{V}_h \times Q_h \text{ such that} \tag{4}$$
$$\begin{cases} a(\boldsymbol{u}_h, \boldsymbol{v}_h) + b(\boldsymbol{v}_h, p_h) = (\boldsymbol{f}, \boldsymbol{v}_h) & \forall \boldsymbol{v}_h \in \boldsymbol{V}_h, \\ b(\boldsymbol{u}_h, q_h) - c_h(p_h, q_h) = 0 & \forall q_h \in Q_h, \end{cases}$$

where $c_h(\cdot,\cdot)$ is the stabilization term, which is a symmetric continuous semi-positive definite bilinear form on Q_h^2. The stabilization term has the general form

$$c_h(p_h,q_h) = \alpha \sum_{K\in\mathcal{T}_h} h_K^2(\nabla p_h,\nabla q_h)_K + \beta \sum_{e\in\mathcal{E}^I} h_e([\![p_h]\!],[\![q_h]\!])_e,$$

where α and β are two non-negative stabilization parameters and $[\![\,\cdot\,]\!]$ denotes the jump operator across the internal edges (faces in three dimensions).

REMARK 1. – A more general form of the stabilization term reads

$$c_h(\boldsymbol{u}_h,p_h;\boldsymbol{v}_h,q_h) = \alpha \sum_{K\in\mathcal{T}_h} h_K^2(-\Delta\boldsymbol{u}_h+\nabla p_h,-\Delta\boldsymbol{v}_h+\nabla q_h)_K + \beta \sum_{e\in\mathcal{E}^I} h_e([\![p_h]\!],[\![q_h]\!])_e.$$

However, since we are planning to use low order elements, the term involving $\Delta\boldsymbol{u}_h$ and $\Delta\boldsymbol{v}_h$ vanishes.

In matrix form Eq. (4) reads

$$\begin{pmatrix} A & B^t \\ B & -C \end{pmatrix}\begin{pmatrix} \boldsymbol{u}_h \\ p_h \end{pmatrix} = \begin{pmatrix} \boldsymbol{f} \\ 0 \end{pmatrix}, \tag{5}$$

where the matrices A, B, and C correspond to the bilinear form $a(\cdot,\cdot)$, $b(\cdot,\cdot)$, and $c_h(\cdot,\cdot)$ respectively.

We consider the following low order pairs of approximation spaces, commonly known as $P_1 - P_0$ and $P_1 - P_1^c$ methods, respectively:

$$\begin{aligned} \boldsymbol{V}_h &= \{\boldsymbol{v}_h \in H_0^1(\Omega)^n : \boldsymbol{v}_{h|_K} \in P_1(K)^n,\ K\in\mathcal{T}_h\} \\ Q_h &= \{q_h \in L_0^2(\Omega) : q_{h|_K} \in P_0(K),\ K\in\mathcal{T}_h\}, \end{aligned} \tag{6}$$

and

$$\begin{aligned} \boldsymbol{V}_h &= \{\boldsymbol{v}_h \in H_0^1(\Omega)^n : \boldsymbol{v}_{h|_K} \in P_1(K)^n,\ K\in\mathcal{T}_h\} \\ Q_h &= \{q_h \in L_0^2(\Omega)\cap H^1(\Omega) : q_{h|_K} \in P_1(K),\ K\in\mathcal{T}_h\}, \end{aligned} \tag{7}$$

where $P_k(K)$ denotes the space of polynomials of the degree at most k on K. The degrees of freedom for the $P_1 - P_0$ and $P_1 - P_1^c$ elements in 2D are depicted in Figures 1, 2, respectively.

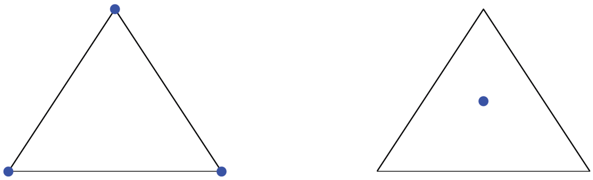

Fig. 1. – Degrees of freedom for the $P_1 - P_0$ element in 2D: velocity left, pressure right.

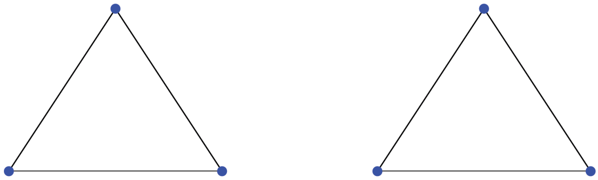

Fig. 2. – Degrees of freedom for the $P_1 - P_1^c$ element in 2D: velocity left, pressure right.

We denote by $B_h : (\boldsymbol{V}_h \times Q_h)^2 \to \mathbb{R}$ the continuous bilinear form associate to the stabilized problem (4), namely

$$B_h(\boldsymbol{u}_h, p_q; \boldsymbol{v}_h, q_h) = a(\boldsymbol{u}_h, \boldsymbol{v}_h) + b(\boldsymbol{v}_h, p_h) + b(\boldsymbol{u}_h, q_h) - c_h(p_h, q_h) \qquad \forall \boldsymbol{u}_h, \boldsymbol{v}_h \in \mathbf{V}_h, \ \forall p_h, q_h \in Q_h,$$

where for low order schemes, like those considered in (6) and (7), the stabilization term is reduced to

$$c_h(p_h, q_h) = \alpha \sum_{K \in \mathcal{T}_h} h_K^2 (\nabla p_h, \nabla q_h)_K + \beta \sum_{e \in \mathcal{E}^I} h_e ([\![p_h]\!], [\![q_h]\!])_e. \tag{8}$$

In the sequel we denote by C a constant independent of h, possibly different at each occurrence and by $\boldsymbol{S}_h$ the following space:

$$\boldsymbol{S}_h = \{\boldsymbol{v} \in \boldsymbol{V} : \boldsymbol{v}_{|_K} \in P_n(K)^n, \ K \in \mathcal{T}_h\},$$

being n the space dimension.

In order to have a well-posed discrete problem, the stabilization parameter β can vanish in the case of continuous pressure approximations, whereas for discontinuous pressure approximations either β is positive or $\boldsymbol{S}_h \subset \boldsymbol{V}_h$.

The next stability theorem indeed holds true (see [13, 12]).

THEOREM 3.1. – *Assume that one of the following conditions is fulfilled:*

(1) $\boldsymbol{S}_h \subset \boldsymbol{V}_h$,
(2) $Q_h \subset C^0(\Omega)$,
(3) $\beta > 0$.

Then for $\alpha > 0$ *the bilinear form* $B_h(\cdot;\cdot)$ *satisfies*

$$\sup_{\substack{(\boldsymbol{v}_h, q_h) \in \boldsymbol{V}_h \times Q_h \\ (\boldsymbol{v}_h, q_h) \neq (0,0)}} \frac{B_h(\boldsymbol{u}_h, p_h; \boldsymbol{v}_h, q_h)}{(\|\boldsymbol{v}_h\|_1^2 + \|q_h\|_0^2)^{1/2}} \geq K_{\alpha,\beta} (\|\boldsymbol{u}_h\|_1^2 + \|p_h\|_0^2)^{1/2} \quad \forall (\boldsymbol{u}_h, p_h) \in \boldsymbol{V}_h \times Q_h, \tag{9}$$

with $K_{\alpha,\beta}$ *constant depending on the stabilization parameters* α *and* β, *but independent of the mesh size* h.

The proof of the stability relies on the following key result: the arguments presented here are partially different from [13].

LEMMA 3.1. – *There exist non-negative constants C_1 and C_2, independent of h, such that*

$$\sup_{\substack{\boldsymbol{v}_h\in\boldsymbol{V}_h\\ \boldsymbol{v}_h\neq 0}} \frac{(\operatorname{div}\boldsymbol{v}_h, q_h)}{\|\boldsymbol{v}\|_1} \geq C_1\|q_h\|_0 - C_2\left(\sum_{K\in\mathcal{T}_h} h_K^2\|\nabla q_h\|_{0,K}^2\right)^{1/2} - C_2\left(\sum_{e\in\mathcal{E}^I} h_e\|[\![q_h]\!]\|_{0,e}^2\right)^{1/2} \qquad \forall q_h\in Q_h.$$

PROOF. – Let $q_h \in Q_h$ be fixed. Then, by the continuous *inf-sup* condition, there exists $\boldsymbol{w} \in \boldsymbol{V}$ such that

$$(\operatorname{div}\boldsymbol{w}, q_h) \geq C_0\|q_h\|_0\|\boldsymbol{w}\|_1.$$

Let $\boldsymbol{w}^{\mathrm{I}} \in \boldsymbol{V}_h$ be the Clément interpolant of $\boldsymbol{w}$ (see [10]). Then it holds

$$\sum_{K\in\mathcal{T}_h} h_K^{-2}\|\boldsymbol{w}-\boldsymbol{w}^{\mathrm{I}}\|_{0,K}^2 + \sum_{e\in\mathcal{E}^I} h_e^{-1}\|\boldsymbol{w}-\boldsymbol{w}^{\mathrm{I}}\|_{0,e}^2 \leq C'\|\boldsymbol{w}\|_1^2$$

and

$$\|\boldsymbol{w}^{\mathrm{I}}\|_1 \leq C''\|\boldsymbol{w}\|_1.$$

Then

$$\begin{aligned}
&\sup_{\substack{\boldsymbol{v}_h\in\boldsymbol{V}_h\\ \boldsymbol{v}_h\neq 0}} \frac{(\operatorname{div}\boldsymbol{v}_h, q_h)}{\|\boldsymbol{v}\|_1} \geq \frac{(\operatorname{div}\boldsymbol{w}^{\mathrm{I}}, q_h)}{\|\boldsymbol{w}^{\mathrm{I}}\|_1} \geq \frac{1}{C''}\frac{(\operatorname{div}\boldsymbol{w}^{\mathrm{I}}, q_h)}{\|\boldsymbol{w}\|_1}\\
&= \frac{1}{C''}\frac{(\operatorname{div}(\boldsymbol{w}^{\mathrm{I}}-\boldsymbol{w}), q_h) + (\operatorname{div}\boldsymbol{w}, q_h)}{\|\boldsymbol{w}\|_1} \geq \frac{1}{C''}\frac{(\operatorname{div}(\boldsymbol{w}^{\mathrm{I}}-\boldsymbol{w}), q_h)}{\|\boldsymbol{w}\|_1} + \frac{C_0}{C''}\|q_h\|_0.
\end{aligned}\tag{10}$$

We then take into account that

$$\begin{aligned}
(\operatorname{div}(\boldsymbol{w}^{\mathrm{I}}-\boldsymbol{w}), q_h) &= \sum_{K\in\mathcal{T}_h}\left\{-(\nabla q_h, \boldsymbol{w}^{\mathrm{I}}-\boldsymbol{w})_K + \int_{\partial K} q_h(\boldsymbol{w}^{\mathrm{I}}-\boldsymbol{w})\cdot\boldsymbol{n}\right\}\\
&= \sum_{K\in\mathcal{T}_h}(\nabla q_h, \boldsymbol{w}-\boldsymbol{w}^{\mathrm{I}})_K + \sum_{e\in\mathcal{E}^I}([\![q_h]\!], \boldsymbol{w}^{\mathrm{I}}-\boldsymbol{w})_e\\
&\geq -\sum_{K\in\mathcal{T}_h}\|\nabla q_h\|_{0,K}\|\boldsymbol{w}-\boldsymbol{w}^{\mathrm{I}}\|_{0,K} - \sum_{e\in\mathcal{E}^I}\|[\![q_h]\!]\|_{0,e}\|\boldsymbol{w}-\boldsymbol{w}^{\mathrm{I}}\|_{0,e}\\
&\geq -\left(\sum_{K\in\mathcal{T}_h} h_K^2\|\nabla q_h\|_{0,K}^2\right)^{1/2}\left(\sum_{K\in\mathcal{T}_h} h_K^{-2}\|\boldsymbol{w}-\boldsymbol{w}^{\mathrm{I}}\|_{0,K}^2\right)^{1/2}\\
&\quad - \left(\sum_{e\in\mathcal{E}^I} h_e\|[\![q_h]\!]\|_{0,e}^2\right)^{1/2}\left(\sum_{e\in\mathcal{E}^I} h_e^{-1}\|\boldsymbol{w}-\boldsymbol{w}^{\mathrm{I}}\|_{0,e}^2\right)^{1/2}\\
&\geq -C'\|\boldsymbol{w}\|_1\left(\sum_{K\in\mathcal{T}_h} h_K^2\|\nabla q_h\|_{0,K}^2\right)^{1/2} - C'\|\boldsymbol{w}\|_1\left(\sum_{e\in\mathcal{E}^I} h_e\|[\![q_h]\!]\|_{0,e}^2\right)^{1/2}.
\end{aligned}\tag{11}$$

By choosing $C_1 = C_0/C''$ and $C_2 = C'/C''$ we obtain the desired result. □

REMARK 2. – If $Q_h \subset C^0(\Omega)$ or $\boldsymbol{S}_h \subset \boldsymbol{V}_h$, then the result of the previous lemma reduces to

$$\sup_{\substack{\boldsymbol{v}_h \in \boldsymbol{V}_h \\ \boldsymbol{v}_h \neq \boldsymbol{0}}} \frac{(\operatorname{div} \boldsymbol{v}_h, q_h)}{\|\boldsymbol{v}\|_1} \geq C_1 \|q_h\|_0 - C_2 \left(\sum_{K \in \mathcal{T}_h} h_K^2 \|\nabla q_h\|_{0,K}^2 \right)^{1/2} \qquad \forall q_h \in Q_h.$$

This is obvious if $Q_h \subset C^0(\Omega)$. For the case $\boldsymbol{S}_h \subset \boldsymbol{V}_h$, we refer to [13, Lemma 3.3].

Although the proof of the Theorem 3.1 is quite standard, we sketch it in order to highlight the dependence of the stability constant on the stabilization parameters.

PROOF. – Let $(\boldsymbol{u}_h, p_h) \in \boldsymbol{V}_h \times Q_h$ be fixed. We look for $(\boldsymbol{v}_h, q_h) \in \boldsymbol{V}_h \times Q_h$ such that

$$\begin{aligned} &B_h(\boldsymbol{u}_h, p_h; \boldsymbol{v}_h, q_h) \geq C(\|\boldsymbol{u}_h\|_1^2 + \|p_h\|_0^2) \\ &(\|\boldsymbol{v}_h\|_1^2 + \|q_h\|_0^2)^{1/2} \leq C(\|\boldsymbol{u}_h\|_1^2 + \|p_h\|_0^2)^{1/2}. \end{aligned} \tag{12}$$

By Lemma 3.1 there exists $\boldsymbol{w}_h \in \boldsymbol{V}_h$ such that:

$$\begin{aligned} &\frac{(\operatorname{div} \boldsymbol{w}_h, p_h)}{\|\boldsymbol{w}_h\|_1} \geq C_1 \|p_h\|_0 - C_2 \left(\sum_{K \in \mathcal{T}_h} h_K^2 \|\nabla p_h\|_{0,K}^2 \right)^{1/2} - C_2 \left(\sum_{e \in \mathcal{E}^I} h_e \|[\![p_h]\!]\|_{0,e}^2 \right)^{1/2} \\ &\|\boldsymbol{w}_h\|_1 = \|p_h\|_0. \end{aligned} \tag{13}$$

Then

$$\begin{aligned} B_h(\boldsymbol{u}_h, p_h; -\boldsymbol{w}_h, 0) &= -(\nabla \boldsymbol{u}_h, \nabla \boldsymbol{w}_h) + (p_h, \operatorname{div} \boldsymbol{w}_h) \\ &\geq -\|\nabla \boldsymbol{u}_h\|_0 \|\nabla \boldsymbol{w}_h\|_0 + C_1 \|p_h\|_0^2 \\ &\quad - C_2 \|p_h\|_0 \left(\sum_{K \in \mathcal{T}_h} h_K^2 \|\nabla p_h\|_{0,K}^2 \right)^{1/2} \\ &\quad - C_2 \|p_h\|_0 \left(\sum_{e \in \mathcal{E}^I} h_e \|[\![p_h]\!]\|_{0,e}^2 \right)^{1/2} \\ &\geq C \Bigg(-\|\nabla \boldsymbol{u}_h\|_0^2 + \|p_h\|_0^2 \\ &\quad - \sum_{K \in \mathcal{T}_h} h_K^2 \|\nabla p_h\|_{0,K}^2 - \sum_{e \in \mathcal{E}^I} h_e \|[\![p_h]\!]\|_{0,e}^2 \Bigg), \end{aligned} \tag{14}$$

where the last inequality stems from Eq. (13) and Young's inequality.

Moreover,

$$B(\boldsymbol{u}_h, p_h; \boldsymbol{u}_h, -p_h) = \|\nabla \boldsymbol{u}_h\|_0^2 + \alpha \sum_{K\in\mathcal{T}_h} h_K^2 \|\nabla p_h\|_{0,K}^2 + \beta \sum_{e\in\mathcal{E}^I} h_e \|[\![p_h]\!]\|_{0,e}^2.$$

Taking $(\boldsymbol{v}_h, q_h) = (\boldsymbol{u}_h - \delta \boldsymbol{w}_h, -p_h)$ we get

$$\begin{aligned}
B_h(\boldsymbol{u}_h, p_h; \boldsymbol{v}_h, q_h) &= B(\boldsymbol{u}_h, p_h; \boldsymbol{u}_h, -p_h) + \delta B_h(\boldsymbol{u}_h, p_h; -\boldsymbol{w}_h, 0) \\
&\geq \|\nabla \boldsymbol{u}_h\|_0^2 + \alpha \sum_{K\in\mathcal{T}_h} h_K^2 \|\nabla p_h\|_{0,K}^2 + \beta \sum_{e\in\mathcal{E}^I} h_e \|[\![p_h]\!]\|_{0,e}^2 \\
&\quad + \delta C(- \|\nabla \boldsymbol{u}_h\|_0^2 + \|p_h\|_0^2 \\
&\quad - \sum_{K\in\mathcal{T}_h} h_K^2 \|\nabla p_h\|_{0,K}^2 - \sum_{e\in\mathcal{E}^I} h_e \|[\![p_h]\!]\|_{0,e}^2).
\end{aligned} \tag{15}$$

Using again Young's inequality and choosing $\delta = \min(1/C, \alpha/C, \beta/C)/2$, we obtain

$$\begin{aligned}
B_h(\boldsymbol{u}_h, p_h; \boldsymbol{v}_h, q_h) &\geq C_{\alpha,\beta}^{(1)} (\|\nabla \boldsymbol{u}_h\|_0^2 + \|p_h\|_0^2 \\
&\quad + \sum_{K\in\mathcal{T}_h} h_K^2 \|\nabla p_h\|_{0,K}^2 + \sum_{e\in\mathcal{E}^I} h_e \|[\![p_h]\!]\|_{0,e}^2) \\
&\geq C_{\alpha,\beta}^{(1)} (\|\nabla \boldsymbol{u}_h\|_0^2 + \|p_h\|_0^2),
\end{aligned} \tag{16}$$

with $C_{\alpha,\beta}^{(1)} = \min(1, \alpha, \beta)/2$. Moreover, it is clear that

$$\left(\|\boldsymbol{v}_h\|_1^2 + \|q_h\|_0^2 \right)^{1/2} \leq C_{\alpha,\beta}^{(2)} \left(\|\boldsymbol{u}_h\|_1^2 + \|p_h\|_0^2 \right)^{1/2},$$

where $C_{\alpha,\beta}^{(2)} = \sqrt{\max(2, 1 + 2\delta^2)}$.

The *inf-sup* constant $K_{\alpha,\beta}$ thus results

$$K_{\alpha,\beta} = \frac{\min(1, \alpha, \beta)}{2\sqrt{\max(2, 1 + 2\delta^2)}}. \tag{17}$$

□

We observe that the stabilized schemes are not consistent. Let $H^1(\mathcal{T}_h) = \{q \in Q : q_{|K} \in H^1(K)\ \forall K \in \mathcal{T}_h\}$. If $p \in H^1(\mathcal{T}_h)$ the consistency error is given by

$$\sup_{q_h\in Q_h} c_h(p, q_h) = \sup_{q_h\in Q_h} \left\{ \alpha \sum_{K\in\mathcal{T}_h} h_K^2 (\nabla p, \nabla q_h)_K + \beta \sum_{e\in\mathcal{E}^I} h_e ([\![p]\!], [\![q_h]\!])_e \right\}. \tag{18}$$

Nevertheless, if $p \in H^{1/2+\varepsilon}(\Omega)$ (for some $\varepsilon > 0$) then, the trace along each edge of the mesh is well-defined, so that the jumps along the interelement edges vanish. Therefore the consistency error given in (18) reduces to the first sum. On the other hand, if $Q_h \subset C^0(\Omega)$ or $\boldsymbol{S}_h \subset \boldsymbol{V}_h$, then β can be chosen equal to zero.

In the case of higher order elements, c_h takes the more general form given in Remark 1; in this case β can be taken equal to zero and the consistency term becomes

$$c_h(\boldsymbol{u}, p; \boldsymbol{v}_h, q_h) = \alpha \sum_{K \in \mathcal{T}_h} h_K^2 (- \Delta \boldsymbol{u} + \nabla p, -\Delta \boldsymbol{v}_h + \nabla q_h)_K.$$

However, in this case, the consistency can be restored by adding at the right hand side of the second equation of problem (4) a suitable term which is given by:

$$\alpha \sum_{K \in \mathcal{T}_h} h_K^2 (\boldsymbol{f}, -\Delta \boldsymbol{v}_h + \nabla q_h)_K. \tag{19}$$

As usual for non-consistent schemes, the error is estimated by the sum of two different contributions related to the approximation and the consistency errors. Indeed from the stability Theorem 3.1, we get by standard techniques the following Strang type result.

THEOREM 3.2. – *Assume that $p \in H^1(\mathcal{T}_h)$ and that one of the following conditions is satisfied:*

(1) $\boldsymbol{S}_h \subset \boldsymbol{V}_h$,
(2) $Q_h \subset C^0(\Omega)$,
(3) $\beta > 0$.

Then for $\alpha > 0$ there exists a constant C, independent of h, such that

$$\begin{aligned}
&\left(\|\boldsymbol{u} - \boldsymbol{u}_h\|_1^2 + \|p - p_h\|_0^2\right)^{1/2} \\
&\quad \le \left(1 + \frac{C}{K_{\alpha,\beta}}\right) \inf_{(\boldsymbol{w}_h, r_h) \in \boldsymbol{V}_h \times Q_h} \Bigg(\|\boldsymbol{u} - \boldsymbol{w}_h\|_1 + \|p - r_h\|_0 \\
&\qquad + \alpha \Big(\sum_{K \in \mathcal{T}_h} h_K^2 \|\nabla (p - r_h)\|_{0,K}^2 \Big)^{1/2} + \beta \Big(\sum_{e \in \mathcal{E}^I} h_e \|[\![p - r_h]\!]\|_{0,e}^2 \Big)^{1/2} \Bigg) \\
&\qquad + \frac{C}{K_{\alpha,\beta}} \sup_{\substack{(\boldsymbol{v}_h, q_h) \in \boldsymbol{V}_h \times Q_h \\ (\|\boldsymbol{v}_h\|_1^2 + \|q_h\|_0^2)^{1/2} = 1}} B_h(\boldsymbol{u} - \boldsymbol{u}_h; p - p_h; \boldsymbol{v}_h; q_h),
\end{aligned} \tag{20}$$

where $K_{\alpha,\beta}$ is the inf-sup constant given in Eq. (17).

PROOF. – As usual, we first estimate the error by triangle inequality

$$\|\boldsymbol{u} - \boldsymbol{u}_h\|_1^2 + \|p - p_h\|_0^2 \le \|\boldsymbol{u} - \boldsymbol{w}_h\|_1^2 + \|\boldsymbol{w}_h - \boldsymbol{u}_h\|_1^2 + \|p - r_h\|_0^2 + \|r_h - p_h\|_0^2 \quad \forall (\boldsymbol{w}_h, r_h) \in \boldsymbol{V}_h \times Q_h. \tag{21}$$

By the discrete *inf-sup* condition (9) there exists $(\bar{\boldsymbol{v}}_h, \bar{q}_h) \in \boldsymbol{V}_h \times Q_h$ such that

$$B_h(\boldsymbol{u}_h - \boldsymbol{w}_h, p_h - r_h; \bar{\boldsymbol{v}}_h, \bar{q}_h) \geq K_{\alpha,\beta}(\|\boldsymbol{u}_h - \boldsymbol{w}_h\|_1^2 + \|p_h - r_h\|_0^2)^{1/2} \tag{22}$$

$$(\|\bar{\boldsymbol{v}}_h\|_1^2 + \|\bar{q}_h\|_0^2)^{1/2} = 1, \tag{23}$$

where $K_{\alpha,\beta}$ is the inf-sup constant given in Eq. (17). Thus

$$\sup_{\substack{(\boldsymbol{v}_h, q_h) \in \boldsymbol{V}_h \times Q_h \\ (\|\boldsymbol{v}_h\|_1^2 + \|q_h\|_0^2)^{1/2} = 1}} B_h(\boldsymbol{u}_h - \boldsymbol{w}_h, p_h - r_h; \boldsymbol{v}_h, q_h) \geq K_{\alpha,\beta}(\|\boldsymbol{u}_h - \boldsymbol{w}_h\|_1^2 + \|p_h - r_h\|_0^2)^{1/2}. \tag{24}$$

It holds

$$B_h(\boldsymbol{u}_h - \boldsymbol{w}_h, p_h - r_h; \boldsymbol{v}_h, q_h) = B_h(\boldsymbol{u}_h - \boldsymbol{u}, p_h - p; \boldsymbol{v}_h, q_h) + B_h(\boldsymbol{u} - \boldsymbol{w}_h, p - r_h; \boldsymbol{v}_h, q_h),$$

where the second term is estimated as follows:

$$\begin{aligned} B_h(\boldsymbol{u} - \boldsymbol{w}_h, p - r_h; \boldsymbol{v}_h, q_h) &\leq \|\nabla(\boldsymbol{u} - \boldsymbol{w}_h)\|_0 \|\nabla \boldsymbol{v}_h\|_0 + \|p - r_h\|_0 \|\boldsymbol{v}_h\|_1 \\ &+ \|\boldsymbol{u} - \boldsymbol{w}_h\|_1 \|q_h\|_0 + \alpha \left(\sum_{K \in \mathcal{T}_h} h_K^2 \|\nabla(p - r_h)\|_{0,K}^2 \right)^{1/2} \left(\sum_{K \in \mathcal{T}_h} h_K^2 \|\nabla q_h\|_{0,K}^2 \right)^{1/2} \\ &+ \beta \left(\sum_{e \in \mathcal{E}^I} h_e \|[\![p - r_h]\!]\|_{0,e}^2 \right)^{1/2} \left(\sum_{e \in \mathcal{E}^I} h_e \|[\![q_h]\!]\|_{0,e}^2 \right)^{1/2}. \end{aligned} \tag{25}$$

By standard scaling argument it holds (see [13])

$$\sum_{K \in \mathcal{T}_h} h_K^2 \|\nabla q_h\|_{0,K}^2 + \sum_{e \in \mathcal{E}^I} h_e \|[\![q_h]\!]\|_{0,e}^2 \leq C \|q_h\|_0^2 \quad \forall q_h \in Q_h. \tag{26}$$

Then since $\|\boldsymbol{v}_h\|_1^2 + \|q_h\|_0^2 = 1$

$$\begin{aligned} B_h(\boldsymbol{u} - \boldsymbol{w}_h, p - r_h; \boldsymbol{v}_h, q_h) \leq C \Bigg(&\|\boldsymbol{u} - \boldsymbol{w}_h\|_1^2 + \|p - r_h\|_0^2 \\ &+ \alpha \sum_{K \in \mathcal{T}_h} h_K^2 \|\nabla(p - r_h)\|_{0,K}^2 + \beta \sum_{e \in \mathcal{E}^I} h_e \|[\![p - r_h]\!]\|_{0,e}^2 \Bigg)^{1/2} \end{aligned} \tag{27}$$

We get the thesis combining Eq. (21), (24), and (27) and taking the inf over $(\boldsymbol{w}_h, r_h) \in \boldsymbol{V}_h \times Q_h$. □

An estimate of the consistency error is given in the next theorem.

THEOREM 3.3. – *Assume that $p \in H^1(\mathcal{T}_h)$. Then there exists a constant C, independent of h, such that*

$$\sup_{\substack{(\boldsymbol{v}_h, q_h) \in \boldsymbol{V}_h \times Q_h \\ (\|\boldsymbol{v}_h\|_1^2 + \|q_h\|_0^2)^{1/2} = 1}} B_h(\boldsymbol{u} - \boldsymbol{u}_h; p - p_h; \boldsymbol{v}_h; q_h) \leq C \left(\alpha h |p|_{1,h} + \beta h^{1/2} \left(\sum_{e \in \mathcal{E}^I} \|[\![p]\!]\|_{0,e}^2 \right)^{1/2} \right), \tag{28}$$

where

$$|p|_{1,h} = \left(\sum_{K\in\mathcal{T}_h} \|\nabla p\|_{0,K}^2\right)^{1/2}.$$

PROOF. – The consistency error is estimated as follows:

$$\begin{aligned}
B_h(\boldsymbol{u}-\boldsymbol{u}_h; p-p_h; \boldsymbol{v}_h; q_h) &= \alpha \sum_{K\in\mathcal{T}_h} h_K^2(\nabla p, \nabla q_h)_K + \beta \sum_{e\in\mathcal{E}^I} h_e([\![p]\!], [\![q_h]\!])_e \\
&\le \alpha \sum_{K\in\mathcal{T}_h} h_K^2 \|\nabla p\|_{0,K}\|\nabla q_h\|_{0,K} + \beta \sum_{e\in\mathcal{E}^I} h_e \|[\![p]\!]\|_{0,e}\|[\![q_h]\!]\|_{0,e} \\
&\le \alpha \left(\sum_{K\in\mathcal{T}_h} h_K^2 \|\nabla p\|_{0,K}^2\right)^{1/2} \left(\sum_{K\in\mathcal{T}_h} h_K^2 \|\nabla q_h\|_{0,K}^2\right)^{1/2} \\
&\quad + \beta \left(\sum_{e\in\mathcal{E}^I} h_e \|[\![p]\!]\|_{0,e}^2\right)^{1/2} \left(\sum_{e\in\mathcal{E}^I} h_e \|[\![q_h]\!]\|_{0,e}^2\right)^{1/2} \\
&\le C\|q_h\|_0 (\alpha h |p|_{1,h} + \beta \left(\sum_{e\in\mathcal{E}^I} h_e \|[\![p]\!]\|_{0,e}^2\right)^{1/2} \quad \forall q_h \in Q_h,
\end{aligned} \tag{29}$$

where the last inequality stems from Eq. (26). Hence we get the result by taking the sup and observing that $\|q_h\|_0 \le 1$. □

REMARK 3. – Notice that if $p \in H^1(\Omega)$, we have $[\![p]\!] = 0$ and the second term in the right hand side of (28) is vanishing. Moreover, $|p|_{1,h} = |p|_1$.

For smooth solution to (2), the following optimal error estimates hold (see [13, 12]).

THEOREM 3.4. – *Assume that the solution* $(\boldsymbol{u}, p)$ *to* (2) *satisfies* $\boldsymbol{u} \in H^2(\Omega)^n$ *and* $p \in H^{l+1}(\Omega)$ *with* $0 \le l \le 1$ *and that one of the following conditions is satisfied:*

(1) $\boldsymbol{S}_h \subset \boldsymbol{V}_h$,
(2) $Q_h \subset C^0(\Omega)$,
(3) $\beta > 0$.

Then for $\alpha > 0$ *the discrete problem* (4) *has a unique solution. Moreover, there exists a constant* $C_{\alpha,\beta}$ *depending on the stabilization parameters but independent of h, such that*

$$\|\boldsymbol{u}-\boldsymbol{u}_h\|_1 + \|p-p_h\|_0 \le C_{\alpha,\beta}(h|\boldsymbol{u}|_2 + h^{l+1}|p|_{l+1} + h|p|_1), \tag{30}$$

being $l = 0$ *for* $P_1 - P_0$ *and* $l = 1$ *for* $P_1 - P_1^c$.

Furthermore, if Ω is convex, we have the following L^2-error estimate

$$\|\boldsymbol{u}-\boldsymbol{u}_h\|_0 \leq \tilde{C}_{\alpha,\beta}(h^2|\boldsymbol{u}|_2 + h^{l+2}|p|_{l+1} + h^2|p|_1), \tag{31}$$

with $\tilde{C}_{\alpha,\beta}$ constant depending on the stabilization parameters but independent of h.

PROOF. – Let $\boldsymbol{u}^{\mathrm{I}}$ and p^{I} denote the interpolants of $\boldsymbol{u}$ and p, respectively. We can take the Clément interpolant of $\boldsymbol{u}$ and the L^2-projection onto piecewise constants or the Clément interpolant of p for P_0 and P_1^c pressure approximations, respectively.

From Theorems 3.2 and 3.3 we have

$$\begin{aligned}\left(\|\boldsymbol{u}-\boldsymbol{u}_h\|_1^2 + \|p-p_h\|_0^2\right)^{1/2} &\leq \left(1+\frac{C}{K_{\alpha,\beta}}\right)\Bigg(\|\boldsymbol{u}-\boldsymbol{u}^{\mathrm{I}}\|_1 + \|p-p^{\mathrm{I}}\|_0 \\ &+ \alpha\Big(\sum_{K\in\mathcal{T}_h} h_K^2\|\nabla(p-p^{\mathrm{I}})\|_{0,K}^2\Big)^{1/2} + \beta\Big(\sum_{e\in\mathcal{E}^I} h_e\|[\![p-p^{\mathrm{I}}]\!]\|_{0,e}^2\Big)^{1/2}\Bigg) \\ &+ \frac{C}{K_{\alpha,\beta}}\left(\alpha h|p|_1 + \beta h^{1/2}\Big(\sum_{e\in\mathcal{E}^I}\|[\![p]\!]\|_{0,e}^2\Big)^{1/2}\right).\end{aligned}$$

Since $p\in H^{l+1}(\Omega)$ then $[\![p]\!]=0$ and the following well-known interpolation estimate holds

$$\Big(\sum_{K\in\mathcal{T}_h} h_K^2\|\nabla(p-p^{\mathrm{I}})\|_{0,K}^2\Big)^{1/2} + \Big(\sum_{e\in\mathcal{E}^I} h_e\|[\![p-p^{\mathrm{I}}]\!]\|_{0,e}^2\Big)^{1/2} \leq Ch^{l+1}|p|_{l+1} \quad \forall p\in H^{l+1}(\Omega).$$

From the last two inequalities we get the result of Eq. (30).

Under the convexity assumption, the L^2-error estimate (31) follows as usual from an Aubin-Nitsche argument. □

Let us consider the case of non smooth pressure solutions, that is $p\in L_0^2(\Omega)\cap H^1(\mathcal{T}_h)$. We have to analyze separately the two finite element choices (6) and (7). Let us start with the P_1-P_0 element. In this case we have that the interpolation error estimate is of optimal order 1, but the stabilized scheme requires $\beta>0$, so that the stabilization term is ($\alpha=0$)

$$c_h(p_h,q_h) = \beta\sum_{e\in\mathcal{E}^I} h_e([\![p_h]\!],[\![q_h]\!])_e.$$

As a consequence we have that the rate of the consistency error is one half, more precisely the error estimate reads

$$
\begin{aligned}
\Big(\|\boldsymbol{u}-\boldsymbol{u}_h\|_1^2+\|p-p_h\|_0^2\Big)^{1/2} &\leq \Big(1+\frac{C}{K_{\alpha,\beta}}\Big)(h|\boldsymbol{u}|_2+h|p|_{1,h}) \\
&+\frac{C}{K_{\alpha,\beta}}\Bigg(\beta h^{1/2}\Big(\sum_{e\in\mathcal{E}^I}\|[\![p]\!]\|_{0,e}^2\Big)^{1/2}\Bigg).
\end{aligned}
\tag{32}
$$

REMARK 4. – The lack of consistency in the case of non smooth pressures produces a suboptimal error bound. Unfortunately, the optimal convergence cannot be restored with a suitable choice of the parameter β (for instance, as a function of the mesh size). Indeed, if $\beta<1$ then $K_{\alpha,\beta}\approx\beta$ and it results

$$
\|\boldsymbol{u}-\boldsymbol{u}_h\|_1+\|p-p_h\|_0\leq C(\beta^{-1}h+h^{1/2}).
$$

On the other hand, if $\beta>1$ then $K_{\alpha,\beta}=C$ independent of h and it results

$$
\|\boldsymbol{u}-\boldsymbol{u}_h\|_1+\|p-p_h\|_0\leq C\beta(h+h^{1/2}).
$$

Hence the rate of convergence is always 1/2.

Concerning the $P_1-P_1^c$ scheme, the rate of convergence is reduced to 1/2 as well in presence of non-smooth pressure solution. In this case we are allowed to take $\beta=0$ in the consistency term, so that the consistency error is of order 1. The suboptimal rate is now due to the estimate of the interpolation error.

4. – Local mass conservation

In the previous sections we studied the convergence properties of stabilized elements. In the application we have in mind, the local mass conservation of the used schemes is a fundamental property. It is clear that mass conservation and convergence are related, but a higher convergence rate does not necessarily mean a better mass conservation.

In this section we consider the issue of mass conservation and discuss possible enhancements of some of the stabilized elements introduced above in the spirit of [4, 3]. The stabilized methods present the drawback that the divergence free constraint is further weakened by the stabilization term which adds a diffusive contribution to the pressure. In [4] the local mass conservation property was obtained by the enrichment of the pressure space with piecewise constants. Obviously, this idea could not help in the case of the P_1-P_0 element; therefore we start by considering the enhanced version of the $P_1-P_1^c$ element.

We consider the following pair of approximation spaces, which we refer to as the $P_1 - (P_1^c + P_0)$ scheme:

$$
\begin{aligned}
\boldsymbol{V}_h &= \{\boldsymbol{v}_h \in H_0^1(\Omega)^n : \boldsymbol{v}_{h|_K} \in P_1(K)^n,\ K \in \mathcal{T}_h\} \\
Q_h &= \{q_h \in L_0^2(\Omega) : q_h = q_1 + q_0, \\
&\qquad q_1 \in C^0(\bar{\Omega}),\ q_{1|_K} \in P_1(K),\ q_{0|_K} \in P_0(K),\ K \in \mathcal{T}_h\}.
\end{aligned} \tag{33}
$$

The degrees of freedom for this element in 2D are depicted in Figure 3.

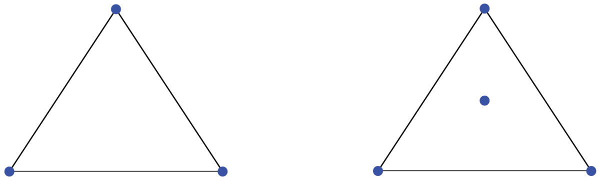

Fig. 3. – Degrees of freedom for the $P_1 - (P_1^c + P_0)$ element in 2D: velocity left, pressure right.

Notice that contrary to the original stabilized scheme both parameters α and β need to be greater than zero: the first one gives the correct stabilization term for the P_1 part of the discrete pressure while the second one takes into account the P_0 part.

We explicitly observe that the result of Lemma 3.1 holds true for the augmented space as well. This is trivial, since the augmented pressure space is still a conforming approximation of the pressure space Q.

As for original stabilized schemes, the stability of the augmented spaces stems from Lemma 3.1.

THEOREM 4.1. – *For $\alpha, \beta > 0$ the bilinear form $B_h(\cdot;\cdot)$ satisfies*

$$
\sup_{\substack{(\boldsymbol{v}_h, q_h) \in \boldsymbol{V}_h \times Q_h \\ (\boldsymbol{v}_h, q_h) \neq (0,0)}} \frac{B_h(\boldsymbol{u}_h, p_h; \boldsymbol{v}_h, q_h)}{(\|\boldsymbol{v}_h\|_1^2 + \|q_h\|_0^2)^{1/2}} \geq K_{\alpha,\beta}(\|\boldsymbol{u}_h\|_1^2 + \|p_h\|_0^2)^{1/2} \quad \forall (\boldsymbol{u}_h, p_h) \in \boldsymbol{V}_h \times Q_h, \tag{34}
$$

with $K_{\alpha,\beta}$ constant depending on the stabilization parameters α and β, but independent of the mesh size h.

PROOF. – The proof is the same as for Theorem 3.1. □

Then from the stability result we get the following optimal order error estimates.

THEOREM 4.2. – *Assume that the solution $(\boldsymbol{u}, p)$ to* (2) *is such that $\boldsymbol{u} \in (H^2(\Omega)^n$ and $p \in H^{s+1}(\Omega)$ with $0 \leq s \leq 1$. Then for $\alpha, \beta > 0$ the discrete problem* (4) *has a unique solution.*

Moreover, there exists a constant $C_{\alpha,\beta}$ depending on the stabilization parameters but independent of h, such that

$$\|\boldsymbol{u} - \boldsymbol{u}_h\|_1 + \|p - p_h\|_0 \le C_{\alpha,\beta}(h|\boldsymbol{u}|_2 + h^{s+1}|p|_{s+1} + h|p|_1). \tag{35}$$

Furthermore, if Ω is convex, we have the following L^2-error estimate

$$\|\boldsymbol{u} - \boldsymbol{u}_h\|_0 \le \tilde{C}_{\alpha,\beta}(h^2|\boldsymbol{u}|_2 + h^{s+2}|p|_{s+1} + h^2|p|_1), \tag{36}$$

with $\tilde{C}_{\alpha,\beta}$ constant depending on the stabilization parameters but independent of h.

PROOF. – The proof is the same as for Theorem 3.4. □

In case of non-smooth pressure solutions, considerations on the reduced rate of convergence similar to those presented in Remark 4 hold for the augmented spaces as well.

REMARK 5. – In Eq. (33) the pressure space Q_h is defined as the sum of two finite element spaces, namely $P_1^c + P_0$. However, it can be easily observed that the sum is not direct, since globally constant functions can be represented exactly by means of piecewise P_0 or continuous P_1 elements.

Concerning the implementation of the method, we avoid the computation of the basis functions of such a finite element by testing the discrete problem (3) with the basis functions of the two subspaces separately. By the above discussion it turns out that matrix B in (5) is rank-deficient, with kernel of dimension 1. On the other hand the matrix C in (5) is positive definite and hence invertible. Thus the global matrix in (5) is invertible.

REMARK 6. – The previous stability and error analysis generalize to higher order stabilized schemes. Thus one might consider the consistent formulation of the $P_2 - P_1^d$ element (quadratic velocity, discontinuous linear pressure) in 2D (with corresponding $P_3 - P_2^d$ element in 3D) stabilized with

$$c_h(\boldsymbol{u}_h, p_h; \boldsymbol{v}_h, q_h) = \alpha \sum_{K \in \mathcal{T}_h} h_K^2(-\Delta\boldsymbol{u}_h + \nabla p_h, -\Delta\boldsymbol{v}_h + \nabla q_h)_K.$$

The advantage of this scheme is twofold. Since there is no jump term in the stabilization, the scheme is consistent. Moreover, thanks to the fact that we consider discontinuous pressure approximations we obtain an element which is locally mass conservative.

As we have seen stability is not an issue for stabilized augmented scheme (33). On the other hand, contrary to Hood-Taylor and Bercovier-Pironneau elements (see [4]), the enhancement with piecewise constant functions does not yield local mass conservative spaces. This is due to the presence of the jump stabilization term (8). In fact, Theorem 3.1 requires $\beta > 0$ for discontinuous pressure approximations and low order velocity spaces.

The presence of the jumps in the stabilization term results in a method which becomes computationally more involved whitout any advantage from the point of view of the mass conservation. Working in two dimensions, in [17, 23, 18] a remedy is proposed for the $P_1 - P_0$ scheme by stabilizing it with *local* jumps. Let us consider a disjoint partition of the mesh $\mathcal{M}_h$ into triangular macroelements M. Each macroelement M is composed by four triangles with vertices at the midpoints of the edges of M. Clearly, it turns out that one of such triangles is completely in the interior of the macroelement. The local stabilized formulation is then based on the introduction of the following discrete bilinear form

$$c_h(p_h, q_h) = \beta \sum_{M \in \mathcal{M}_h} \sum_{e \in \mathcal{E}^I_{\mathcal{M}}} h_e(\llbracket p_h \rrbracket, \llbracket q_h \rrbracket)_e, \tag{37}$$

where $\mathcal{E}^I_{\mathcal{M}}$ is the set of the edges which lie in the interior of each $M \in \mathcal{M}_h$.

In [18] the inf-sup condition has been proved. In fact, with this approach we are essentially considering a $P_1 isoP_2$ velocity space. The pressure function on a macroelement can be decomposed into the sum of a constant plus a piecewise constant. Therefore to get the stability of the scheme we can observe that the constant on the macroelement is controlled by the $P_1 isoP_2$ velocity space, while for the piecewise constant inside the macroelement the local stabilization term works. This local stabilization procedure has the advantage that the local mass conservation is preserved at the macroelement level. Infact choosing q_h to be the characteristic function of $M \in \mathcal{M}$ into the second equation of (4) we have that $c_h(p_h, q_h) = 0$ so that

$$b(\boldsymbol{u}_h, q_h) = \int_M \operatorname{div} \boldsymbol{u}_h d\boldsymbol{x} = 0.$$

Hence the average of the divergence vanishes on each macroelement.

Indeed, a more general element has been considered in [17, 23, 18]: the macroelement M does not need to be a triangle; the vertices of the subtriangles can be moved and the macroelement M deformed as long as the topology of the mesh does not change. Such element may become important, for instance, when evolution problems involve mesh deformations.

In order to achieve local mass conservation for the choice (7), we introduce the following stabilized element which, up to the authors knowledge, is new and is closely related to the idea of enhancing the pressure space using piecewise constants [4]. We denote by $\mathcal{T}_{h/2}$ the mesh obtained by $\mathcal{T}_h$ joining the midpoints of the internal edges. We consider the following augmented approximation spaces in $2D$, which we name $P_1 isoP_2 - (P_1 isoP_2 + P_0)$:

$$\boldsymbol{V}_h = \{\boldsymbol{v}_h \in H_0^1(\Omega)^2 : \boldsymbol{v}_{h|_K} \in P_1(K)^2,\ K \in \mathcal{T}_{h/2}\}$$

(38) $$Q_h = \{q_h \in L_0^2(\Omega) : q_h = q_1 + q_0,\ q_1 \in C^0(\bar{\Omega}),\ q_{1|_K} \in P_1(K)\ K \in \mathcal{T}_{h/2},\ q_{0|_K} \in P_0(K),\ K \in \mathcal{T}_h\}.$$

Both the velocity and the pressure spaces are of Bercovier-Pironneau type (see [1]). Moreover, the pressure space is enriched by adding piecewise constant functions on the coarse mesh $\mathcal{T}_h$. The degrees of freedom for this element in 2D are depicted in Figure 4.

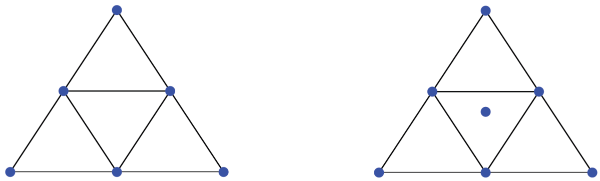

Fig. 4. – Degrees of freedom for the $P_1 isoP2 - (P_1 isoP_2 + P_0)$ element in 2D: velocity left, pressure right.

In this case the stabilization term is given by

$$c_h(p_h, q_h) = \alpha \sum_{K \in \mathcal{T}_{h/2}} h_K^2 (\nabla p_h, \nabla q_h)_K,$$

which stabilizes the piecewise linear part of the pressure. On the other hand, since the $P_1 isoP_2$ velocity element is closely related to the P_2 element on the coarse mesh, there is no need to consider jump stabilization. This is one of the advantages of this method since the absence of jump terms allows to use a standard assembling process.

As for the schemes previously considered, the stability of this method is a consequence of Lemma 3.1, which in this case reads: there exist non-negative constants C_1 and C_2, independent of h, such that

$$\sup_{\substack{\boldsymbol{v}_h \in \boldsymbol{V}_h \\ \boldsymbol{v}_h \neq \boldsymbol{0}}} \frac{(\operatorname{div} \boldsymbol{v}_h, q_h)}{\|\boldsymbol{v}\|_1} \geq C_1 \|q_h\|_0 - C_2 \left(\sum_{K \in \mathcal{T}_{h/2}} h_K^2 \|\nabla q_h\|_{0,K}^2 \right)^{1/2}.$$

We notice that the term with the jumps in this case is not necessary because the space $P_1 isoP_2$ has the same degrees of freedom as P_2, so that the proof of [13] works also in the present situation.

Then following the same lines of the proof of Theorem 3.1, we obtain the next stability theorem:

THEOREM 4.3. – *The bilinear form $B_h(\cdot;\cdot)$ satisfies*

$$\sup_{\substack{(\boldsymbol{v}_h,q_h)\in\boldsymbol{V}_h\times Q_h\\(\boldsymbol{v}_h,q_h)\neq(\boldsymbol{0},0)}}\frac{B_h(\boldsymbol{u}_h,p_h;\boldsymbol{v}_h,q_h)}{\|\boldsymbol{v}_h\|_1+\|q_h\|_0}\geq K_\alpha(\|\boldsymbol{u}_h\|_1^2+\|p_h\|_0^2)^{1/2},\quad\forall(\boldsymbol{u}_h,p_h)\in\boldsymbol{V}_h\times Q_h\tag{39}$$

with K_α constant depending on α but independent of h.

Finally, from the stability result we get as before the following optimal order error estimates.

THEOREM 4.4. – *Assume that the solution $(\boldsymbol{u},p)$ to* (2) *satisfies the following regularity assumptions $\boldsymbol{u}\in H^2(\Omega)^2$ and $p\in H^{s+1}(\Omega)$ with $0\leq s\leq 1$. Then for $\alpha>0$ the discrete problem* (4) *has a unique solution.*

Moreover, there exists a constant C_α depending on the stabilization parameter but independent of h, such that

$$\|\boldsymbol{u}-\boldsymbol{u}_h\|_1+\|p-p_h\|_0\leq C_\alpha(h|\boldsymbol{u}|_2+h^{s+1}|p|_{s+1}+h|p|_1).\tag{40}$$

Furthermore, if Ω is convex, we have the following L^2-error estimate

$$\|\boldsymbol{u}-\boldsymbol{u}_h\|_0\leq\tilde{C}_\alpha(h^2|\boldsymbol{u}|_2+h^{s+2}|p|_{s+1}+h^2|p|_1),\tag{41}$$

with $\tilde{C}_\alpha$ constant depending on α but independent of h.

We observe that even if the pressure is not smooth $p\in L^2_0(\Omega)\cap H^1(\mathcal{T}_h)$, we obtain the optimal rate 1. In fact, referring to the discussion at the end of Sect. 3, we observe that despite the presence of discontinuities in the pressure there is no need to add a stabilization term containing the interelement jumps. This term in the P_1-P_0 and in the $P_1-(P_1^c+P_0)$ cases caused a consistency error of order 1/2. On the other hand the piecewise constant contribution to the pressure space allows us to get the optimal interpolation error which could not be achieved for the $P_1-P_1^c$ element.

REMARK 7. – As for the $P_1-(P_1^c+P_0)$ element (see Remark 5), the pressure space Q_h in (38) is defined as the sum of two finite element spaces, namely $P_1isoP_2+P_0$. Also in this case the sum is not direct, since globally constant functions can be represented exactly by means of piecewise P_0 or continuous P_1isoP_2 elements. Concerning the implementation of the method, we still avoid the computation of the basis functions of such a finite element by testing the discrete problem (3) with the basis functions of the two subspaces separately. However in this case, both the matrices B and C in (5) are rank-deficient. As for the $P_1-(P_1^c+P_0)$ element, the kernel of the matrix B has dimension one, whilst in this case the matrix C is only positive semidefinite and has the following form:

$$\mathrm{C} = \left(\begin{array}{c|c} \mathrm{X} & 0 \\ \hline 0 & 0 \end{array}\right).$$

The square diagonal block X is the contribution to C of the basis functions of the $P_1 isoP_2$ pressure element, while the square null block 0 is that of the P_0 element. By the above discussion it turns out that the global matrix in (5) is rank-deficient, with kernel of dimension 1. We shall give precise details on the way we deal with this issue in the solution of the linear system (5) in the next section.

Let us consider the issue of the mass conservation. As before let us take q_h the characteristic function of an element $K \in \mathcal{T}_h$ in the second equation of (4). Since $c_h(p_h, q_h) = 0$ we obtain again that the average of divergence of the velocity vanishes on each element of the coarse mesh $\mathcal{T}_h$.

Concluding, this element shows very appealing properties: it is easy to implement, it enjoys the stability, optimal order convergence and local mass conservation properties.

5. – Numerical experiments

This section is devoted to numerical experiments. In particular the following schemes will be tested:

- $P_1 - P_1^c$. This is a reference stabilized low order finite element (see Figure 2).
- $P_1 - P_0$. It is here considered as the simplest possible stabilized element (see Figure 1).
- $P_1 - P_1^c + P_0$. It is studied in order to explore a P_0 enrichment of the $P_1 - P_1^c$, in the same manner as we intended enriching Bercovier-Pironneau and Hood-Taylor finite elements in [4] (see Figure 3).
- $P_1 isoP_2 - P_1 isoP_2 + P_0$. We introduce this finite element in order to circumvent the pressure jump stabilization term and preserve the mass conservation properties of piecewise P_0 functions (see Figure 4).
- $P_1 isoP_2 - P_1^c + P_0$ The augmented Bercovier-Pironneau finite element is stable and mass preserving, then it is here considered as a performance standard (see Figure 5).

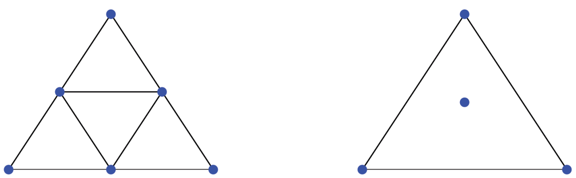

Fig. 5. – Degrees of freedom for the $P_1 isoP_2 - (P_1 + P_0)$ element in 2D: velocity left, pressure right.

For each scheme we will evaluate the convergence properties, the approximation results, and the mass conservation results. A first set of experiments will involve a continuous solution for the pressure:

$$\begin{aligned} u_x &= \cos(2\pi x)\sin(2\pi y) + \sin(2\pi y), \\ u_y &= \sin(2\pi x)\cos(2\pi y) - \sin(2\pi x), \\ p &= 2\pi(\cos(2\pi x)) + 2\pi(\cos(2\pi y)), \\ \boldsymbol{f} &= -\Delta \boldsymbol{u} + \nabla p. \end{aligned} \tag{42}$$

A second set of experiments will be carried out considering a discontinuous pressure solution, which has the following form:

$$p = \begin{cases} 2\pi(\cos(2\pi x)) + 2\pi(\cos(2\pi y)) + 5 & \text{for } x \geq 1/2 \\ 2\pi(\cos(2\pi x)) + 2\pi(\cos(2\pi y)) - 5 & \text{for } x < 1/2. \end{cases}$$

5.1 – *Convergence properties*

Table 1 represents the convergence error for the $P_1 - P_1^c$ finite element tested on the *continuous* solution case. Convergence orders for velocity, both in L^2 and H^1 norms, are optimal, and so is the order for the divergence. The L^2 norm of the pressure error shows a super-convergent behavior in a similar way as noticed in [4], for the Bercovier-Pironneau finite element. It is remarkable and would deserve further investigation the fact that indeed this behavior has been noticed on non structured meshes as well. Tables 2 and 3 report the orders of convergence for $P_1 - P_0$ and $P_1 - (P_1^c + P_0)$ finite elements, which, as expected, are optimal. The comparison between $P_1 - P_1^c$ and $P_1 + (P_1^c + P_0)$ shows that the enhancement to the pressure space prevents the super-convergence for the pressure. An analogous behavior was observed in [4] for the Bercovier-Pironneau finite element, in the sense that, when we add the piecewise constant functions, the superconvergence is not showing up anymore. However, even if we

TABLE 1. –Spatial convergence for the $P_1 - P_1^c$ finite element, $\alpha = 0.1$. Continuous solution test case.

h_x	$\lVert p - p_h \rVert_{L^2}$		$\lVert \boldsymbol{u} - \boldsymbol{u}_h \rVert_{L^2}$		$\lVert \nabla(\boldsymbol{u} - \boldsymbol{u}_h) \rVert_{L^2}$		$\lVert \operatorname{div} \boldsymbol{u}_h \rVert_{L^2}$	
	Error	Rate	Error	Rate	Error	Rate	Error	Rate
1/8	8.374e–01	–	1.328e–01	–	2.791e+00	–	1.617e+00	–
1/16	2.915e–01	1.5	3.521e–02	1.9	1.421e+00	1.0	8.590e–01	0.9
1/32	9.200e–02	1.7	8.952e–03	2.0	7.127e–01	1.0	4.355e–01	1.0
1/64	2.853e–02	1.7	2.249e–03	2.0	3.564e–01	1.0	2.183e–01	1.0
1/128	9.003e–03	1.7	5.630e–04	2.0	1.781e–01	1.0	1.091e–01	1.0

(All columns under the spanning header $P_1 - P_1^c$.)

TABLE 2. –Spatial convergence for the $P_1 - P_0$ finite element, $\beta = 0.1$. Continuous solution test case.

h_x	$\|p - p_h\|_{L^2}$		$\|\boldsymbol{u} - \boldsymbol{u}_h\|_{L^2}$		$\|\nabla(\boldsymbol{u} - \boldsymbol{u}_h)\|_{L^2}$		$\|\mathrm{div}\,\boldsymbol{u}_h\|_{L^2}$	
	Error	Rate	Error	Rate	Error	Rate	Error	Rate
1/8	2.163e+00	–	1.675e–01	–	2.820e+00	–	1.571e+00	–
1/16	1.003e+00	1.1	4.527e–02	1.9	1.424e+00	1.0	8.507e–01	0.9
1/32	4.823e–01	1.1	1.155e–02	2.0	7.125e–01	1.0	4.339e–01	1.0
1/64	2.375e–01	1.0	2.901e–03	2.0	3.562e–01	1.0	2.179e–01	1.0
1/128	1.180e–01	1.0	7.261e–04	2.0	1.781e–01	1.0	1.090e–01	1.0

TABLE 3. – Spatial convergence for the $P_1 - (P_1^c + P_0)$ finite element, $\alpha = 0.1,\ \beta = 0.1$. Continuous solution test case.

h_x	$\|p - p_h\|_{L^2}$		$\|\boldsymbol{u} - \boldsymbol{u}_h\|_{L^2}$		$\|\nabla(\boldsymbol{u} - \boldsymbol{u}_h)\|_{L^2}$		$\|\mathrm{div}\,\boldsymbol{u}_h\|_{L^2}$	
	Error	Rate	Error	Rate	Error	Rate	Error	Rate
1/8	1.852e+00	–	1.655e–01	–	2.807e+00	–	1.555e+00	–
1/16	8.242e–01	1.2	4.406e–02	1.9	1.421e+00	1.0	8.485e–01	0.9
1/32	3.856e–01	1.1	1.116e–02	2.0	7.122e–01	1.0	4.336e–01	1.0
1/64	1.872e–01	1.0	2.797e–03	2.0	3.562e–01	1.0	2.179e–01	1.0
1/128	9.239e–02	1.0	6.991e–04	2.0	1.781e–01	1.0	1.090e–01	1.0

are loosing the superconvergence for the pressure, the enhancement to the pressure space has been introduced in order to improve the local mass conservation properties of the finite elements. We shall discuss this aspect later on in this section.

We now discuss the convergence properties for the *discontinuous* pressure test case. We first consider Table 4, and notice that the discon-

TABLE 4. – Spatial convergence for the $P_1 - P_1^c$ finite element, $\alpha = 0.1$. Discontinuous solution test case.

h_x	$\|p - p_h\|_{L^2}$		$\|\boldsymbol{u} - \boldsymbol{u}_h\|_{L^2}$		$\|\nabla(\boldsymbol{u} - \boldsymbol{u}_h)\|_{L^2}$		$\|\mathrm{div}\,\boldsymbol{u}_h\|_{L^2}$	
	Error	Rate	Error	Rate	Error	Rate	Error	Rate
1/8	1.505e+00	–	1.431e–01	–	2.926e+00	–	1.824e+00	–
1/16	9.735e–01	0.6	3.969e–02	1.8	1.570e+00	0.9	1.081e+00	0.8
1/32	6.771e–01	0.5	1.108e–02	1.8	8.628e–01	0.9	6.496e–01	0.7
1/64	4.770e–01	0.5	3.237e–03	1.8	4.981e–01	0.8	4.094e–01	0.7
1/128	3.369e–01	0.5	1.001e–03	1.7	3.048e–01	0.7	2.698e–01	0.6

TABLE 5. – Spatial convergence for the $P_1 - P_0$ finite element with respect to $\beta/[\![p]\!]$. Discontinuous pressure test case.

h_x		$\beta = 10$	$\beta = 1$	$\beta = 0.1$	$\beta = 0.02$	$\beta = 0.01$
		$\\|\nabla(\boldsymbol{u} - \boldsymbol{u}_h)\\|_{L^2}$ Convergence Rate				
1/16	1/32	0.81	0.92	0.98	1.03	−28.74
1/32	1/64	0.93	0.76	0.96	1.01	−131.78
1/64	1/128	0.72	0.65	0.92	1.00	−10.83
1/128	1/256	0.56	0.58	0.87	0.99	−84.56
1/256	1/512	0.52	0.54	0.79	0.98	NaN
		$\\|\boldsymbol{u} - \boldsymbol{u}_h\\|_{L^2}$ Convergence Rate				
1/16	1/32	1.03	1.68	1.95	1.94	−26.00
1/32	1/64	1.50	1.78	1.94	1.99	−130.82
1/64	1/128	1.74	1.75	1.91	2.00	−9.78
1/128	1/256	1.77	1.69	1.85	2.00	−83.34
1/256	1/512	1.72	1.62	1.77	1.99	NaN
		$\\|p - p_h\\|_{L^2}$ Convergence Rate				
1/16	1/32	0.79	1.03	0.97	0.98	−30.80
1/32	1/64	1.04	0.76	0.88	1.00	−130.36
1/64	1/128	0.87	0.59	0.79	0.99	−12.25
1/128	1/256	0.61	0.54	0.70	0.96	−82.56
1/256	1/512	0.53	0.52	0.62	0.93	NaN

tinuity of the pressure solution prevents the $P_1 - P_1^c$ from performing optimal rates. Tables 5 and 6 represent the rate of convergence for various choices of the stabilization parameter β for $P_1 - P_0$ and $P_1 - (P_1^c + P_0)$ elements. Where the stabilization parameter is not large enough to guarantee the stability of the element we filled the corresponding entry of the table with a *NaN*. For non smooth solution we proved that the error decreases as $h^{1/2}$. Table 5, 6 numerically demonstrate the error estimates. In order to comment on the results we first focus on Table 5 where the results for the $P_1 - P_0$ element are reported. These numerical results could be misleading, in fact a superficial interpretation of Table 5 could suggest that there exists a value for β that recovers the optimal convergence rate. In Section 3 we proved that this is not the case (see Remark 4). Figure 7(a) makes the situation clearer. We can see that when h is relatively large the

TABLE 6. – Spatial convergence for the $P_1 - (P_1^c + P_0)$ finite element with respect to $\beta/[\![p]\!]$ and $\alpha = 0.1$. Discontinuous pressure test case.

h_x		$\beta = 10$	$\beta = 1$	$\beta = 0.1$	$\beta = 0.02$	$\beta = 0.01$
			$\|\nabla(\boldsymbol{u} - \boldsymbol{u}_h)\|_{L^2}$ Convergence Rate			
1/16	1/32	0.87	0.90	0.98	1.03	1.09
1/32	1/64	0.80	0.84	0.97	1.01	–18.60
1/64	1/128	0.71	0.76	0.94	1.00	–53.82
1/128	1/256	0.64	0.67	0.89	1.00	–73.11
1/256	1/512	0.58	0.61	0.82	1.00	NaN
			$\|\boldsymbol{u} - \boldsymbol{u}_h\|_{L^2}$ Convergence Rate			
h_x		$\beta = 10$	$\beta = 1$	$\beta = 0.1$	$\beta = 0.02$	$\beta = 0.01$
1/16	1/32	1.86	1.89	1.97	1.95	1.90
1/32	1/64	1.80	1.84	1.97	1.99	–15.42
1/64	1/128	1.72	1.76	1.94	2.00	–52.84
1/128	1/256	1.64	1.67	1.90	2.00	–72.29
1/256	1/512	1.58	1.61	1.83	2.00	NaN
			$\|p - p_h\|_{L^2}$ Convergence Rate			
h_x		$\beta = 10$	$\beta = 1$	$\beta = 0.1$	$\beta = 0.02$	$\beta = 0.01$
1/16	1/32	0.56	0.59	0.92	0.99	0.94
1/32	1/64	0.51	0.52	0.79	1.01	–18.56
1/64	1/128	0.50	0.51	0.69	1.01	–53.78
1/128	1/256	0.50	0.50	0.61	1.00	–73.04
1/256	1/512	0.50	0.50	0.56	1.00	NaN

convergence error is of first order and this is compatible with the error estimate (32): in this case the first term

$$\left(1 + \frac{C}{K_{\alpha,\beta}}\right) h(|\boldsymbol{u}|_2 + |p|_{1,h})$$

is dominant with respect to

$$\frac{C}{K_{\alpha,\beta}} \left(\beta h^{1/2} \left(\sum_{e \in \mathcal{E}^I} \|[\![p]\!]\|_{0,e}^2 \right)^{1/2} \right).$$

The opposite situation occurs as h decreases where the second term prevails and the rate of convergence turns to 1/2. As a consequence, we can state, that the

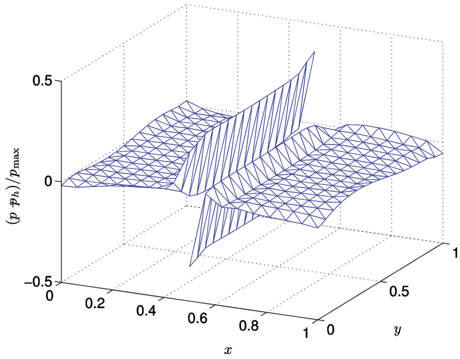

(a) $P_1 - P_1^c$, $\alpha = 0.1$.

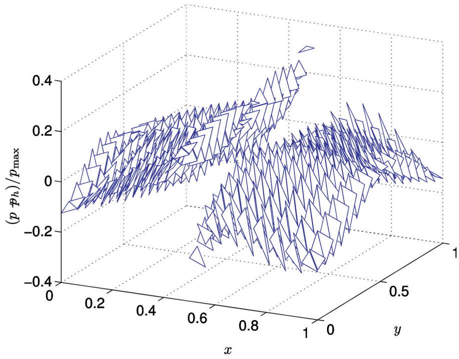

(b) $P_1 - P_0$, $\beta = 0.7$.

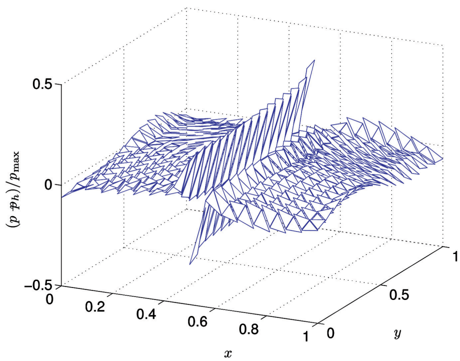

(c) $P_1 - (P_1^c + P_0)$, $\alpha = 0.1$, $\beta = 0.7$.

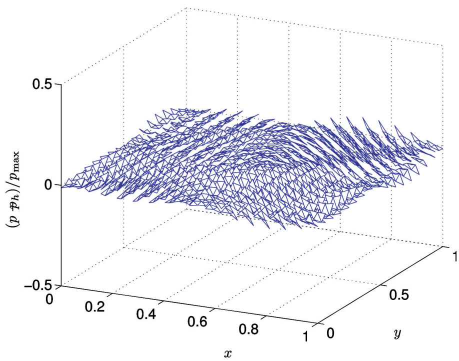

(d) $P_1 isoP_2 - (P_1 isoP_2 + P_0)$, $\alpha = 0.1$.

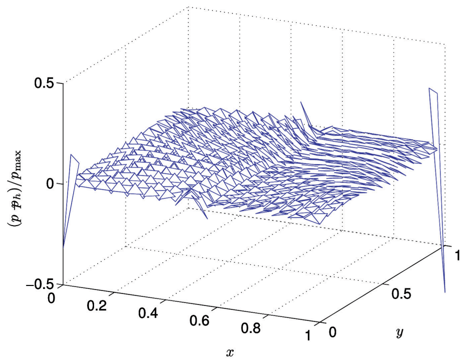

(e) $P_1 isoP_2 - (P_1^c + P_0)$.

Fig. 6. – Pressure error for the finite elements, discontinuous test case.

TABLE 7. – Spatial convergence for the $P_1 isoP_2 - (P_1 isoP_2 + P_0)$ finite element, $\alpha = 0.1$. Continuous solution test case.

h_x	$P_1 isoP_2 - (P_1 isoP_2 + P_0)$ $\|p - p_h\|_{L^2}$		$\|\boldsymbol{u} - \boldsymbol{u}_h\|_{L^2}$		$\|\nabla(\boldsymbol{u} - \boldsymbol{u}_h)\|_{L^2}$		$\|\mathrm{div}\, \boldsymbol{u}_h\|_{L^2}$	
	Error	Rate	Error	Rate	Error	Rate	Error	Rate
1/8	1.154e+00	–	3.495e–02	–	2.387e+00	–	1.236e+00	–
1/16	5.744e–01	1.0	9.436e–03	1.9	1.214e+00	1.0	6.440e–01	0.9
1/32	2.858e–01	1.0	2.467e–03	1.9	6.104e–01	1.0	3.263e–01	1.0
1/64	1.425e–01	1.0	6.382e–04	2.0	3.057e–01	1.0	1.639e–01	1.0
1/128	7.117e–02	1.0	1.643e–04	2.0	1.530e–01	1.0	8.210e–02	1.0

error for lowest-order, β-stabilized finite elements goes to zero only as $h^{1/2}$ when the solution is characterized by a discontinuity. The same observations apply to the $P_1 - (P_1^c + P_0)$ element; Table 6 shows the convergence rate with respect to β. Figure 7(b)demonstrates, that, no matter the choice of β, as h decreases the rate of convergence is dominated by $h^{1/2}$.

Since we just demonstrated that the the pressure jump stabilization term affects the convergence characteristics of the scheme, we introduced the $P_1 isoP_2 - (P_1 isoP_2 + P_0)$ finite element. In this case the P_0 component of the pressure is controlled by the interelement velocity degree of freedom and does not need the pressure jump stabilization term. This is the reason why it can recover optimal convergence rates for *discontinuous* pressure solution. In fact the convergence rates are the same as for the *continuous* case, see Tables 7 and 8, respectively.

TABLE 8. – Spatial convergence for the $P_1 isoP_2 - (P_1 isoP_2 + P_0)$ finite element, $\alpha = 0.1$. Discontinuous solution test case.

h_x	$P_1 isoP_2 - (P_1 isoP_2 + P_0)$ $\|p - p_h\|_{L^2}$		$\|\boldsymbol{u} - \boldsymbol{u}_h\|_{L^2}$		$\|\nabla(\boldsymbol{u} - \boldsymbol{u}_h)\|_{L^2}$		$\|\mathrm{div}\, \boldsymbol{u}_h\|_{L^2}$	
	Error	Rate	Error	Rate	Error	Rate	Error	Rate
1/8	1.154e+00	–	3.495e–02	–	2.387e+00	–	1.236e+00	–
1/16	5.744e–01	1.0	9.436e–03	1.9	1.214e+00	1.0	6.440e–01	0.9
1/32	2.858e–01	1.0	2.467e–03	1.9	6.104e–01	1.0	3.263e–01	1.0
1/64	1.425e–01	1.0	6.382e–04	2.0	3.057e–01	1.0	1.639e–01	1.0
1/128	7.114e–02	1.0	1.644e–04	2.0	1.530e–01	1.0	8.210e–02	1.0

5.2 – *Approximation of pressure discontinuities*

On the other hand, fluid-structure interaction problems arising in biological models are often characterized by fluid domains separated by thin membranes, resulting in a discontinuous solution for the pressure. This is the reason why Figure 6 represents the relative error for the pressure $\|p - p_h\|_{L^2}/\max(p)$ for different finite elements for the *discontinuous* solution test case. The errors in Figure 6(e) at $(0, 0)$ and $(1, 1)$ are due the mesh requirement we explored in [4] that is not satisfied by the used mesh.

The $P_1 - P_1^c$ finite element in Figure 6(a) is affected by a Gibbs phenomenon. If we only look at the approximation properties of the involved spaces, the $P_1 - P_0$ element (see Figure 6(b)) is expected to capture such a discontinuity, but the stabilization term, involving the pressure jump between two elements, is a continuity factor, causing the Gibbs phenomenon to appear. This is also related to the consistency error that has been discussed in the previous sections and we shall confirm numerically later in this section.

Figure 6(c) suggests that the behavior of the $P_1 - (P_1^c + P_0)$ element is mostly driven by the continuous component of the pressure space. The last finite element we implemented, the $P_1 isoP_2 - (P_1 isoP_2 + P_0)$, finally shows good performance and no Gibbs phenomenon. We believe it is important to remark that this scheme is characterized by the same mesh for the velocity and the pressure, which we consider a nice feature from the applicative perspective, and by a piecewise constant function that has no need for the stabilization term involving the parameter β. Since we do not need a stabilization term for the piecewise constant function, the discontinuity in the solution for the pressure is reconstructed with an error comparable to the one observed for the augmented Bercovier-Pironneau finite element. Moreover the $P_1 isoP_2 - (P_1 isoP_2 + P_0)$ element shows no restriction on the mesh.

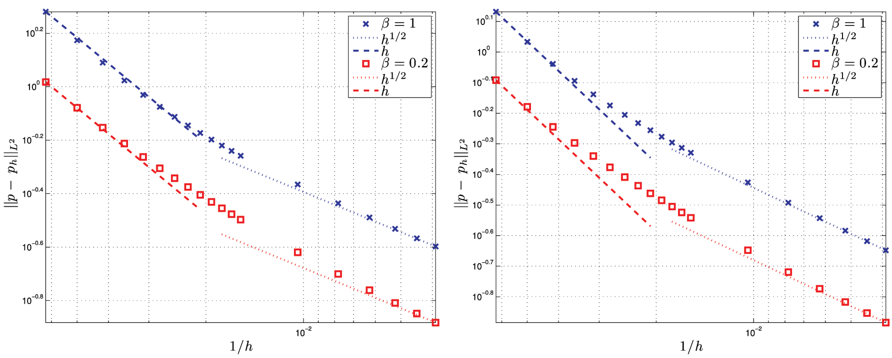

(a) $P_1 - P_0$. (b) $P_1 - (P_1^c + P_0)$, $\alpha = 0.1$.

Fig. 7. – Convergence rates for $P_1 - P_0$ and $P_1 - (P_1^c + P_0)$ with respect to β. Notice that the consistency error is causing the convergence rate to deteriorate.

5.3 – *Mass conservation performances*

We now turn to the fundamental question of local mass conservation of the element we have implemented. In order to do so, we would like to plot the divergence of the discrete velocity vectorfield, averaged on suitably chosen (local) subdomains. It is opinion of the authors that a fair comparison between P_1 velocity elements and $P_1 isoP_2$ velocity elements is performed with the same degrees of freedom for the velocity, and not considering the same value of h. In order to do so, we will plot the macroelementwise averaged divergence:

$$\mathrm{avg}_M(\mathrm{div}\,\boldsymbol{u}_h) = \frac{1}{M}\int_M \mathrm{div}\,\boldsymbol{u}_h\ d\boldsymbol{x} \qquad \forall M \in \mathcal{M}_h, \tag{43}$$

for the P_1 velocity elements (where M is composed of four triangles as in the mesh for the $P_1 isoP_2$ element). For the $P_1 isoP_2$ velocity elements we plot the elementwise averaged divergence:

$$\mathrm{avg}_K(\mathrm{div}\,\boldsymbol{u}_h) = \frac{1}{K}\int_K \mathrm{div}\,\boldsymbol{u}_h\ d\boldsymbol{x} \qquad \forall K \in \mathcal{T}_h.$$

It should be noticed that equation (43) plays the role of a smoothing procedure. In this way, we are giving the P_1 velocity elements a little advantage in our mass conservation competition. Results are represented in Figure 8. As proved by Figures 8(a), 8(b), and 8(c), the corresponding $P_1 - P_1^c$, $P_1 - P_0$ and P_1- $(P_1^c + P_0)$, finite elements are characterized by a non zero value of the real divergence, moreover they are affected by higher divergence values nearby the discontinuity. Nevertheless the little advantage we gave these elements, the resulting schemes are not mass preserving. On the other hand $P_1 isoP_2-$ $(P_1 isoP_2 + P_0)$, as expected, shows numerically zero value for the averaged divergence for each $K \in \mathcal{T}_h$, see Figure 8(d). For the sake of completeness, we report in Figure 8(e) similar conservation results obtained with the augmented Bercovier-Pironneau finite element, which has been analyzed in [4]. In consideration of this result, in combination with the convergence results previously presented, we are reassured in defining as mass preserving the $P_1 isoP_2-$ $(P_1 isoP_2 + P_0)$ finite element.

We conclude the section devoted to numerical experiments with a final remark. The intersection between $P_1 isoP_2$ and P_0 spaces is the global constant function over Ω, the resulting B^t matrix is not full rank, and C cannot compensate this deficiency, as explained in Remark 7, Section 4. In [4] we tackled this issue with a QR factorization for rank deficient matrices. Here we show that it is sufficient to set one P_0 basis function to zero to set the intersection to the null element.

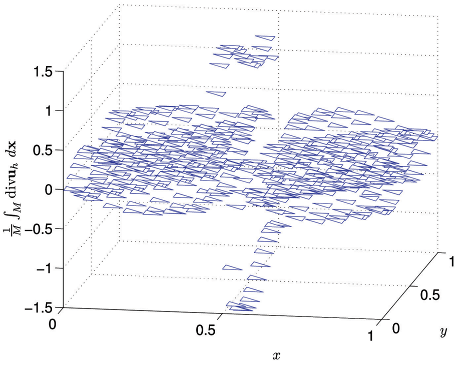

(a) $P_1 - P_1^c$, $\alpha = 0.1$.

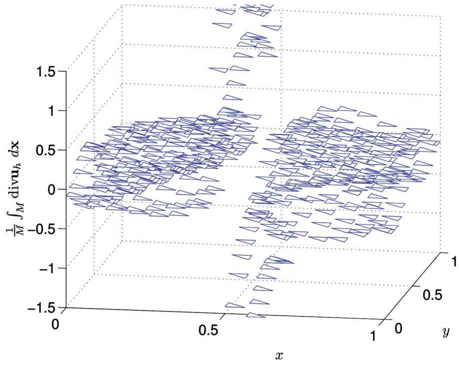

(b) $P_1 - P_0$, $\beta = 0.7$.

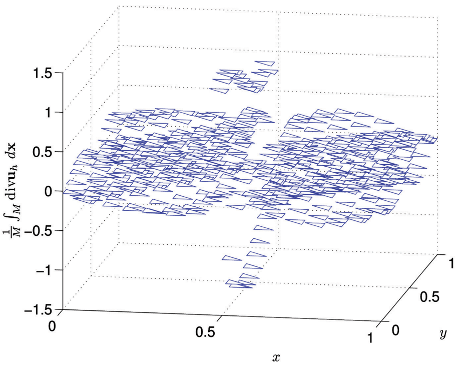

(c) $P_1 - (P_1^c + P_0)$, $\alpha = 0.1$, $\beta = 0.7$.

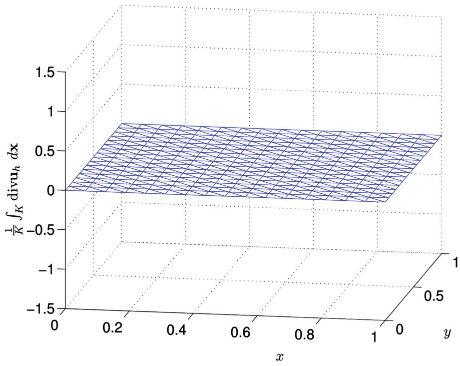

(d) $P_1 isoP_2 - (P_1 isoP_2 + P_0)$, $\alpha = 0.1$.

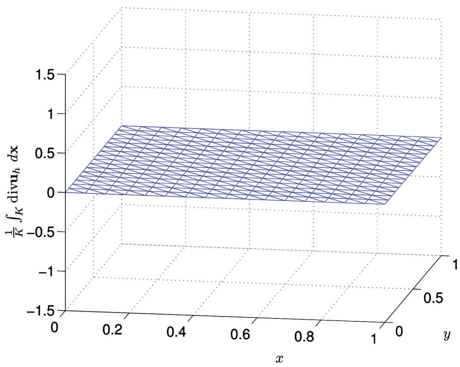

(e) $P_1 isoP_2 - (P_1^c + P_0)$.

Fig. 8. – Divergence for the finite elements, discontinuous test case.

6. – Conclusions

As mentioned in the preceding lines, our interest in studying pressure discontinuous finite elements is motivated by the necessity of approximating phenomena driven by mass conservation properties of the finite element, and by their capabilities of interpolating discontinuous pressure solutions. With the stability analysis and the numerical experiments, we demonstrated that both the $P_1 - P_0$ and $P_1 - (P_1^c + P_0)$ do not represent feasible choice for the numerical representation of phenomena characterized by discontinuous pressure. On the one hand, the plot of the error, Figure 6, suggests that the stabilization term involving the interelement pressure jump introduces some continuity in between elements which can produce a Gibbs phenomenon in the approximation of nonsmooth pressures. One the other hand, the performance of these elements is also affected by a consistency error that prevents to recover optimal rate of convergence, see Tables 5, 6, and Figure 7.

A newly implemented scheme, the $P_1 isoP_2 - (P_1 isoP_2 + P_0)$ element, allows us to avoid the suboptimal convergence arising from the consistency term, to obtain very satisfactory local conservation properties, and to optimally approximate jumping pressures.

This element is characterized by several feasible properties. First, we demonstrated, it provides satisfactory results in the approximation of discontinuous pressure solution, and it is mass preserving, see Figures 6(d), and 8(d). It relies on the same mesh for the velocity and the pressure. It is easy to implement since it does not need a stabilization term of the form:

$$c_h(p_h, q_h) = \beta \sum_{e \in \mathcal{E}^I} h_e([\![p_h]\!], [\![q_h]\!])_e$$

which is characterized by a non standard assembling procedure. Moreover the implementation of $P_1 isoP_2 - (P_1 isoP_2 + P_0)$ can be achieved simply acting on the numbering of the equations for the P_0 functions. This means adding a piecewise constant to every $k_i \in \mathcal{T}_{h/2}$ and setting the same equation number $\forall k_i \subset K \in \mathcal{T}_h$. Numerical experiments demonstrate that this element recover optimal rates of convergence in approximating discontinuous pressure solutions. The interpolation of the discontinuity in the pressure is sharp and the averaged divergence of the discrete velocity is numerically zero.

REFERENCES

[1] M. BERCOVIER - O. PIRONNEAU, *Error estimates for finite element method solution of the Stokes problem in the primitive variables*, Numer. Math., **33** (2) (1979), 211-224.

[2] D. BOFFI - F. BREZZI - M. FORTIN, *Finite elements for the Stokes problem*. In D. Boffi and L. Gastaldi, editors, Mixed finite elements, compatibility conditions, and applica-

tions, volume 1939 of Lecture Notes in Mathematics (Springer-Verlag, Berlin, 2008), 45-100.

[3] D. BOFFI - N. CAVALLINI - F. GARDINI - L. GASTALDI, *Immersed boundary method: performance analysis of popular finite element spaces*. In M. Papadrakakis, E. Onate and B. Schrefler, editors, COUPLED PROBLEMS 2011. Computational Methods for Coupled Problems in Science and Engineering IV (Cimne, 2011).

[4] D. BOFFI - N. CAVALLINI - F. GARDINI - L. GASTALDI, *Local Mass Conservation of Stokes Finite Elements*, J. Sci. Comput., to appear.

[5] D. BOFFI - N. CAVALLINI - L. GASTALDI, *Finite element approach to immersed boundary method with different fluid and solid densities.*, Math. Models Methods Appl. Sci., **21** (12) (2011), 2523–2550.

[6] D. BOFFI - L. GASTALDI - L. HELTAI - C. S. PESKIN, *On the hyper-elastic formulation of the immersed boundary method*,Comput. Methods Appl. Mech. Engrg., **197** (25-28) (2008), 2210-2231.

[7] F. BREZZI - M. FORTIN, *Mixed and hybrid finite element methods*, volume 15 of Springer Series in Computational Mathematics (Springer-Verlag, New York, 1991).

[8] F. BREZZI - J. PITKÄRANTA, *On the stabilization of finite element approximations of the Stokes equations*. In Efficient solutions of elliptic systems (Kiel, 1984), volume 10 of Notes Numer. Fluid Mech. (Vieweg, Braunschweig, 1984), 11-19.

[9] P. G. CIARLET, *The finite element method for elliptic problems*, North-Holland Publishing Co. (Amsterdam, 1978).

[10] P. CLÉMENT, *Approximation by finite element functions using local regularization*, Rev. Française Automat. Informat. Recherche Opérationnelle Sér. Rouge Anal. Numér., **9** (R-2) (1975), 77-84.

[11] M. CREMONESI - A. FRANGI - U. PEREGO, *A Lagrangian finite element approach for the analysis of fluid-structure interaction problems*, Internat. J. Numer. Methods Engrg., **84** (5) (2010), 610-630.

[12] L. P. FRANCA - T. J. R. HUGHES - R. STENBERG, *Stabilized finite element methods*. In Incompressible computational fluid dynamics: trends and advances (Cambridge Univ. Press, Cambridge, 2008), 87-107.

[13] L. P. FRANCA - R. STENBERG, *Error analysis of Galerkin least squares methods for the elasticity equations*, SIAM J. Numer. Anal., **28** (6) (1991), 1680-1697.

[14] T. J. R. HUGHES - L. P. FRANCA, *A new finite element formulation for computational fluid dynamics. VII. The Stokes problem with various well-posed boundary conditions: symmetric formulations that converge for all velocity/pressure spaces*, Comput. Methods Appl. Mech. Engrg., **65** (1) (1987), 85-96.

[15] T. J. R. HUGHES - L. P. FRANCA - M. BALESTRA, *Errata: "A new finite element formulation for computational fluid dynamics. V. Circumventing the Babuška-Brezzi condition: a stable Petrov-Galerkin formulation of the Stokes problem accommodating equal-order interpolations"*, Comput. Methods Appl. Mech. Engrg., **62** (1) (1987), 111.

[16] S. R. IDELSOHN - E. OÑATE, *The challenge of mass conservation in the solution of free-surface flows with the fractional-step method: problems and solutions*, Int. J. Numer. Methods Biomed. Eng., **26** (10) (2010), 1313-1330.

[17] N. KECHKAR - D. J. SILVESTER, *The stabilisation of low order mixed finite element methods for incompressible flow*. In Proceedings of the Fifth International Symposium on Numerical Methods in Engineering, Vol. 1, 2 (Lausanne, 1989) (Southampton, 1989), 111-116. Comput. Mech.

[18] N. KECHKAR - D. J. SILVESTER, *Analysis of locally stabilized mixed finite element methods for the Stokes problem*, Math. Comp., **58** (197) (1992), 1-10.

[19] P. Le Tallec - J. Mouro, *Fluid structure interaction with large structural displacements*, Comput. Methods Appl. Mech. Engrg., **190** (2001), 3039-3067.
[20] G. Matthies - L. Tobiska, *Mass conservation of finite element methods for coupled flow-transport problems*, Int. J. Comput. Sci. Math., **1** (2-4) (2007), 293-307.
[21] C. Michler - E. H. van Brummelen - S. J. Hulshoff - R. de Borst, *The relevance of conservation for stability and accuracy of numerical methods for fluid-structure interaction*, Comput. Methods Appl. Mech. Engrg., **192** (2003), 4195-4215.
[22] P. Ryzhakov - E. Oñate - R. Rossi - S. Idelsohn, *Improving mass conservation in simulation of incompressible flows*, Int. J. Numer. Meth. Engng. (2012).
[23] D. J. Silvester - N. Kechkar, *Stabilised bilinear-constant velocity-pressure finite elements for the conjugate gradient solution of the Stokes problem*, Comput. Methods Appl. Mech. Engrg., **79** (1) (1990), 71-86.

Daniele Boffi, Dipartimento di Matematica “F. Casorati”,
Università degli Studi di Pavia, via Ferrata 1, I-27100 Pavia, Italy
E-mail: daniele.boffi@unipv.it

Nicola Cavallini, Dipartimento di Matematica “F. Casorati”,
Università degli Studi di Pavia, via Ferrata 1, I-27100 Pavia, Italy
E-mail: nicola.cavallini@unipv.it

Francesca Gardini, Dipartimento di Matematica “F. Casorati”,
Università degli Studi di Pavia, via Ferrata 1, I-27100 Pavia, Italy
E-mail: francesca.gardini@unipv.it

Lucia Gastaldi, Dipartimento di Matematica,
Università di Brescia, via Valotti 9, I-25133 Brescia, Italy
E-mail: lucia.gastaldi@ing.unibs.it

Received April 19, 2012 and in revised form June 26, 2012